

Agulhas Leakage Predominantly Responds to the Southern Hemisphere Westerlies

JONATHAN V. DURGADOO

GEOMAR Helmholtz Centre for Ocean Research Kiel, Kiel, Germany

BENJAMIN R. LOVEDAY AND CHRIS J. C. REASON

Department of Oceanography, University of Cape Town, Cape Town, South Africa

PIERRICK PENVEN

LMI ICEMASA, LPO, UMR 6523 (CNRS, IFREMER, IRD, UBO), Brest, France

ARNE BIASTOCH

GEOMAR Helmholtz Centre for Ocean Research Kiel, Kiel, Germany

(Manuscript received 22 February 2013, in final form 27 May 2013)

ABSTRACT

The Agulhas Current plays a crucial role in the thermohaline circulation through its leakage into the South Atlantic Ocean. Under both past and present climates, the trade winds and westerlies could have the ability to modulate the amount of Indian–Atlantic inflow. Compelling arguments have been put forward suggesting that trade winds alone have little impact on the magnitude of Agulhas leakage. Here, employing three ocean models for robust analysis—a global coarse-resolution, a regional eddy-permitting, and a nested high-resolution eddy-resolving configuration—and systematically altering the position and intensity of the westerly wind belt in a series of sensitivity experiments, it is shown that the westerlies, in particular their intensity, control the leakage. Leakage responds proportionally to the intensity of westerlies up to a certain point. Beyond this, through the adjustment of the large-scale circulation, energetic interactions occur between the Agulhas Return Current and the Antarctic Circumpolar Current that result in a state where leakage no longer increases. This adjustment takes place within one or two decades. Contrary to previous assertions, these results further show that an equatorward (poleward) shift in westerlies increases (decreases) leakage. This occurs because of the redistribution of momentum input by the winds. It is concluded that the reported present-day leakage increase could therefore reflect an unadjusted oceanic response mainly to the strengthening westerlies over the last few decades.

1. Introduction

The climatically relevant component of the Agulhas Current (AC) system is arguably its inflow into the South Atlantic Ocean (de Ruijter et al. 1999). One of the unique features of this western boundary current system is that it redistributes heat and salt not only poleward but also equatorward in the form of Agulhas leakage (AL; Fig. 1). The equatorward injection of warm salty thermocline waters into the Atlantic forms a major part

of the return flow toward the North Atlantic, where, through active air–sea interactions at high latitudes, deep waters are formed (Gordon 1986; Gordon et al. 1992; Cunningham and Marsh 2010). In this way, the Agulhas system is considered to be important for global climate (Beal et al. 2011), and as a result the variability of Agulhas leakage on all time scales is of particular interest. In the past, some evidence for leakage reduction during glacial times (Peeters et al. 2004), possibly modulated by a northward migration of the subtropical front south of Africa (Bard and Rickaby 2009), has been inferred from sediment records. At glacial terminations, increase in leakage has been further linked with the recovery of the Atlantic thermohaline circulation (Knorr and Lohmann 2003). Under the current (and future) warming climate,

Corresponding author address: Jonathan Durgadoo, GEOMAR Helmholtz Centre for Ocean Research Kiel, Düsternbrooker Weg 20, 24105 Kiel, Germany.
E-mail: jdurgadoo@gmail.com

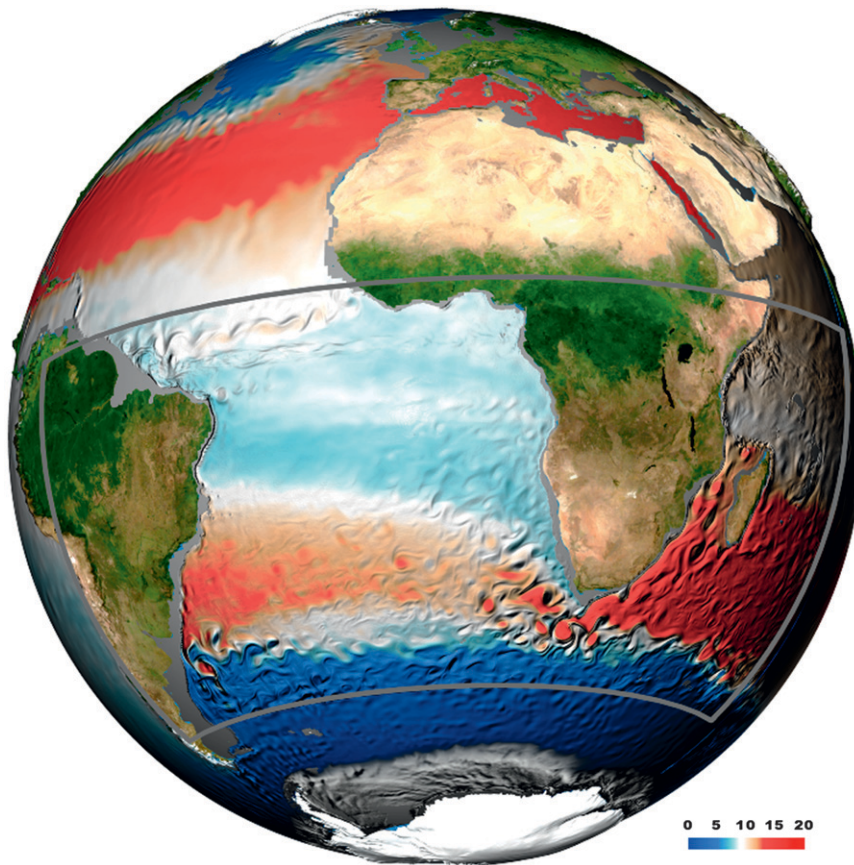


FIG. 1. Mid-depth (250–400 m) temperature (shading; °C) and velocity gradients (shown as the three-dimensional-depth expression) in a 5-day-average snapshot centered at 17 Jun 2006 from the hindcast realization of INALT01 illustrating the major pathway of Agulhas leakage across the South Atlantic. The INALT01 configuration consists of a global half-degree model with a tenth-degree nest over the region demarcated by the gray box (50°S–8°N, 70°W–70°E).

model studies suggest an increasing trend in Agulhas leakage (Biaostoch et al. 2009b; Rouault et al. 2009) that results in an overall salinification of the South Atlantic (Biaostoch and Böning 2013). The effectiveness of this significant exchange south of Africa for the most part is thought to be linked in one way or another to the wind patterns of the Southern Hemisphere (Biaostoch et al. 2009b; Rouault et al. 2009).

The Agulhas system is sandwiched between two major wind belts, namely the southeast trades, between the equator and about 30°S, and the westerlies, over roughly 30°–60°S. With the average latitudinal range of the positive wind stress curl region in the Indian Ocean extending beyond the termination of the African continent near 34°S (Marshall and Plumb 2007), the Agulhas Current leaves the continental slope as a free jet. An interplay between its large inertia and the position of the zero wind stress curl (maximum westerlies) leads to its retroflection (Ou and de Ruijter 1986), a process that

also determines the amount of leakage into the Atlantic (de Ruijter et al. 1999; Pichevin et al. 1999; Dijkstra and de Ruijter 2001). Therefore, the variability of Agulhas leakage on all time scales is expected to be connected to the strength and/or position of trades and/or westerlies.

The trade winds are largely responsible for the inertia of the Agulhas Current. Rouault et al. (2009) and van Sebille et al. (2009) [who used the same model as Biaostoch et al. (2009b)] found the contemporary increase in leakage to be linked with the upstream strength of the Agulhas Current. Within their range of model observations, they disagreed, however, on the sign of the relationship; Rouault et al. (2009) claimed an increase in leakage caused by increase in Agulhas Current, while van Sebille et al. (2009) argued for a decrease in the upstream inertia that leads to an increase in leakage. Both of these studies implied that the trade winds influence leakage magnitude. In a series of realistic global and regional ocean–sea ice models, Loveday et al. (2013, manuscript

submitted to *J. Phys. Oceanogr.*) showed that the sensitivity of Agulhas leakage to the Agulhas Current transport decreases with increasing horizontal resolution. In the eddy-resolving simulations, large changes in the upstream transport of the Agulhas Current had almost no effect on the magnitude of the leakage. Even though a stronger Agulhas transport did cause the Agulhas Current to break from the shelf farther upstream (Ou and de Ruijter 1986), the inertial jet always proceeded southwestward. As a result, despite large localized changes in both mean and eddy kinetic energy (EKE), the annual mean retroflection position remained stable, consistent with observed present-day (Dencausse et al. 2010) and reconstructed past (Franzese et al. 2009) measurements, and Agulhas leakage is unaffected. The increase in kinetic energy possibly leads to a recently described turbulent retroflection regime (Le Bars et al. 2012) where leakage is no longer dependent on the incoming transport.

Given this apparent decoupling between Agulhas leakage and trade winds, in this study we explore the possible dependency of leakage on the Southern Hemisphere westerlies. We systematically alter the position and magnitude of the westerly wind belt within three model configurations similar to those used by Biastoch et al. (2009b) and van Sebille et al. (2009) (half-degree global, with and without a tenth-degree nest) and Rouault et al. (2009) (quarter-degree regional) in order to achieve robust results. The strategy we employ generally follows the works of Oke and England (2004), Sijp and England (2008, 2009), and Biastoch and Böning (2013). The models are all forced by the same atmospheric data and consistent diagnostics are derived. In doing so, we aim to disentangle the relationship between the magnitude of Agulhas leakage and the location and strength of westerlies.

Following a description of the models and of our experiment strategy in section 2, we explore the equilibrium (section 3) and transient (section 4) leakage response to change in westerlies. In section 5, we seek a mechanism explaining the results. Then, we discuss the implications in section 6 before summarizing our main findings in section 7.

2. Model configurations and experiment strategy

The three models employed in this study are ORCA05, INALT01, and AGIO. The first two—based on the ocean/sea ice Nucleus for European Modelling of the Ocean, version 3.1.1 (NEMO v3.1.1; Madec 2008), and developed under the Drakkar framework (The Drakkar Group 2007)—are global models and will be described first. AGIO, summarized thereafter, is a regional model based on the Regional Ocean Modeling System (ROMS; Shchepetkin and McWilliams 2005) and described

thoroughly in Loveday et al. (2013, manuscript submitted to *J. Phys. Oceanogr.*). Similar configurations of these models were used by Biastoch et al. (2009b), Rouault et al. (2009), and van Sebille et al. (2009) but with different setups and forcing fields, which we hypothesize have led to their conflicting results. To assess this, we performed all experiments under the same atmospheric forcing with as much coherence and conformity as possible.

a. ORCA05 and INALT01

Both ORCA05 (coarse-resolution configuration) and INALT01 (nested configuration) follow an ORCA setup (Madec and Imbard 1996; Barnier et al. 2006). In this setup, a tripolar horizontal grid is used and south of 20°N the grid is Mercator type. Variables are staggered following an Arakawa-C arrangement. In the vertical, the model uses z coordinates with a total of 46 levels (10 levels in the top 100 m and a maximum of 250-m resolution at depth). To enhance representation of flow near bottom topography, the deepest grid box is allowed to be partially filled (Barnier et al. 2006) in addition to a nonlinear bottom friction (Tréguier 1992). A free-slip lateral momentum boundary condition is used. The treatment of tracers is implemented using a Laplacian operator for the lateral diffusion and the total variance dissipation (Zalesak 1979) scheme for advection. Lateral diffusion on momentum uses a bi-Laplacian operator with a vector form advection scheme that conserves energy and enstrophy (Arakawa and Hsu 1990). Subgrid-scale vertical mixing is calculated explicitly through the turbulent eddy kinetic dependent diffusion scheme (Blanke and Delecluse 1993).

ORCA05, with half-degree nominal horizontal resolution, which in the Agulhas region is ~ 45 km, is an established configuration at successfully reproducing large-scale global circulation (Biastoch et al. 2008a). INALT01 consists of a base global model (that is identical in configuration to ORCA05) and a nest embedded within between 50°S–8°N and 70°W–70°E (Fig. 1). The nest refines the horizontal model grid over the Agulhas Current system and South Atlantic fivefold to a tenth degree (~ 9 km over the Agulhas region). This also implies a fourfold time-stepping refinement from 36 (base) to 9 (nest) minutes. Bathymetry within the nest region is interpolated from 2-Minute Gridded Global Relief Data (ETOPO2v2; <http://www.ngdc.noaa.gov/mgg/global/relief/ETOPO2/ETOPO2v2-2006/ETOPO2v2g/>).

The horizontal refinement is achieved by adopting the Adaptive Grid Refinement in Fortran (AGRIF) (Debreu and Blayo 2008) approach whereby both model grids are coupled in a two-way mode at every base model time step to provide the nest with open boundary conditions from the base but also enabling the mesoscale

dynamics of the nest to permeate into the base. For this reason, neither the base of INALT01 nor ORCA05 has parameterized mesoscale eddies, a practice that is usually common for models of such resolution class. Eddy parameterization, such as the Gent and McWilliams (1990) scheme, typically mimics the impact of eddies on tracer fluxes as isopycnal diffusion and eddy advection. This has an overall effect of reducing isopycnal steepness. Such parameterization is believed to dampen the influence of the mesoscale dynamics of the nest onto the base. ORCA05 was also run without eddy parameterization in order to allow consistent comparison between both models.

INALT01 is an update of AG01 (Biaostoch et al. 2009a), which has been demonstrated to represent the dynamics of the Agulhas Current and its large-scale impact successfully (Biaostoch et al. 2008b,c, 2009a,b; van Sebille et al. 2009). With its wider high-resolution domain encompassing the South Atlantic basin as well as the tropical Atlantic, INALT01 better lends itself to the investigation of the hypothesized impact of Agulhas leakage on the Atlantic heat, freshwater, and momentum balances. In addition, the advective pathways between the Agulhas system and the North Atlantic can be further explored. The new configuration simulates successfully two major western boundary currents of the Southern Hemisphere.

Prescribing appropriate atmospheric forcing is crucial for ocean modeling. The Common Ocean–Ice Reference Experiments, version 2b (CORE v2b; Large and Yeager 2009), provides the necessary coherent and globally balanced dataset to drive the model. Through bulk formulation, 6-hourly air–sea fluxes of heat, freshwater, and momentum; daily short- and longwave radiation; and monthly rain and snow are used in conjunction with surface ocean temperatures and velocities, which effectively allow some feedback between ocean and atmosphere. For this study, both climatologically and interannually varying CORE fields were used.

Ocean-only models often exhibit drifts in properties. To constrict such artificial drifts within ORCA05 and INALT01, a 10% precipitation reduction (which falls within the CORE dataset uncertainty range) north of 55°N is implemented in addition to a sea surface salinity restoring over the top 50 m with a time scale of 8.3 years. This very weak salt flux damping is capped at $0.5 \text{ kg m}^{-1} \text{ s}^{-1}$ to prevent regions of strong gradients from being excessively damped.

Initializing the thermohaline fields with a combined dataset from Levitus *World Ocean Atlas 1998* (<http://www.esrl.noaa.gov/psd/>) and Polar Science Center Hydrographic Climatology (Steele et al. 2001), and starting from rest, ORCA05 is allowed to spin up for 20 years forced with interannually (1978–97) varying CORE

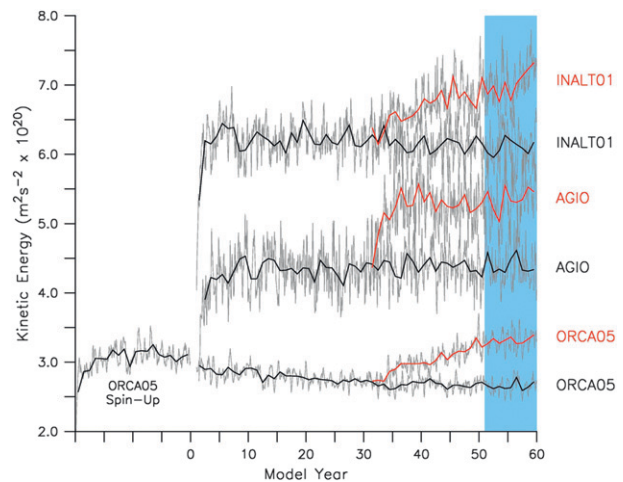


FIG. 2. Volume-integrated (10° – 45° S, 10° W– 60° E) kinetic energy per unit mass ($\text{m}^2 \text{s}^{-2}$) with annual values (thick lines) overlaying monthly values (gray). Following a 20-yr spinup, reference (REF; black lines) experiments were performed for all three models. Wind anomalies were added from year 31; an example of the SHW+40% (red lines) runs is shown. For the purpose of clarity, INALT01 values are offset by $1 \times 10^{20} \text{ m}^2 \text{ s}^{-2}$. Common analysis period (model years 51–60) for Fig. 6 is indicated by the blue shading.

fields. This strategy promotes a stable Atlantic meridional overturning circulation with a reasonable magnitude of $\sim 18 \text{ Sv}$ ($1 \text{ Sv} \equiv 10^6 \text{ m}^3 \text{ s}^{-1}$) (Cunningham and Marsh 2010) that, in the previous version (AG01), was $\sim 10 \text{ Sv}$ (Biaostoch et al. 2008b). Dynamic equilibrium is reached within the 20 years of spinup (Fig. 2), and this output is then used to warm start the experiments outlined in section 2c.

b. AGIO

The AGIO configuration (Loveday et al. 2013, manuscript submitted to *J. Phys. Oceanogr.*) is a quarter-degree-resolution eddy-permitting implementation of ROMS (Shchepetkin and McWilliams 2005), constructed using ROMSTOOLS (Penven et al. 2008). The domain, which extends from 48° S to 7° N and from 29° W to 115° E on a Mercator grid, spans the Indian and southeast Atlantic basins. AGIO is an extension of the South African Experiment (SAfE) configuration (Penven et al. 2006), which was used by Rouault et al. (2009). The average grid spacing over the southern Agulhas region is $\sim 23 \text{ km}$. The vertical resolution in AGIO is described by 32 σ -coordinate levels following the General Bathymetric Chart of the Oceans with 1° resolution (GEBCO1; http://www.gebco.net/data_and_products/gridded_bathymetry_data/)-derived bathymetry and stretched toward the surface. The regional bathymetry is selectively smoothed to reduce pressure gradient errors (Haidvogel and Beckmann 1999). Higher-order numerics and a

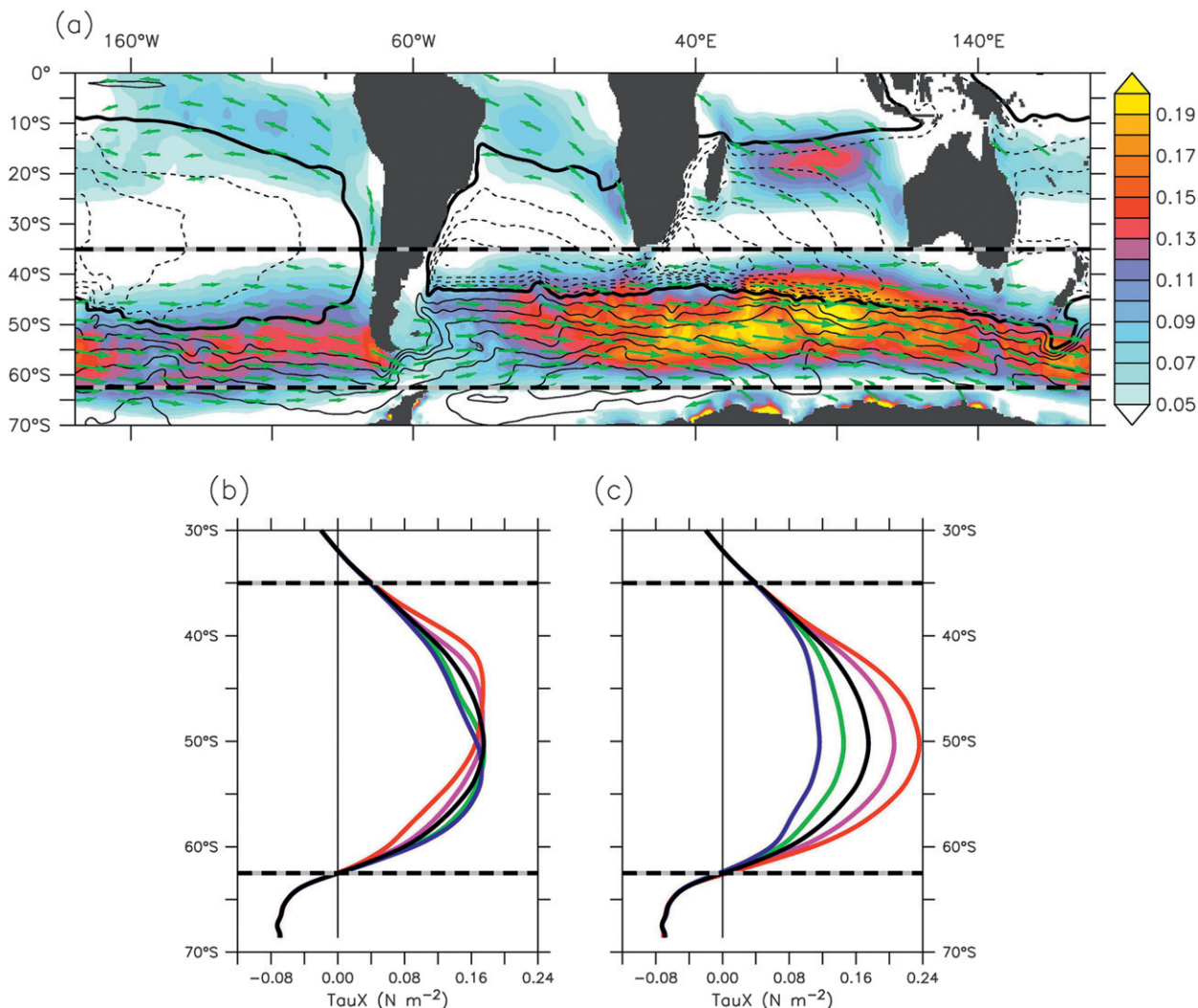


FIG. 3. (a) Wind stress magnitude (shading; N m^{-2}) and direction (vector) with horizontal barotropic streamfunction contour overlay [data extracted from ORCA05-REF experiment; contour intervals are 10 and 25 Sv for negative (dashed line) and positive (full lines) values, respectively; thick contour represents the zero line]. Zonally averaged (20° – 115°E) wind stress (N m^{-2}) with thick black curve indicating the time-reference case: (b) westerly position altered by -4° (blue), -2° (green), $+2^{\circ}$ (pink), and $+4^{\circ}$ (red) about the mean (black), without changing the total energy input; and (c) intensity change by -40% (blue), -20% (green), $+20\%$ (pink), and $+40\%$ (red) of the mean (black). Wind changes are applied within the region 35° – 63°S .

third-order, upstream-biased advection scheme reduce dispersion, allowing steep density gradients to be preserved, and enhancing precision for a given resolution (Shchepetkin and McWilliams 1998). The splitting of diffusion and advection via the Rotated, Split-Upstream 3rd Order (RSUP3) scheme minimizes spurious diapycnal mixing (Marchesiello et al. 2009). Western boundary currents are selectively damped via a parameterization of horizontal viscosity (Smagorinsky 1963) and subgrid-scale vertical mixing follows a nonlocal K -profile parameterization (Large et al. 1994). The lateral viscosity and diffusion are zero in the domain interior and increase to $1000 \text{ m}^2 \text{ s}^{-1}$ in the sponge layer within $\sim 200 \text{ km}$ of the

domain boundaries. Prognostic variables are connected to the external conditions by an active radiation scheme (Marchesiello et al. 2001). Lateral boundary conditions for all AGIO experiments are derived from the climatological monthly mean ORCA05 reference experiment, and variability associated with the Antarctic Circumpolar Current (ACC) is thereby excluded. AGIO is initialized with outputs from the ORCA05 20-yr spinup.

c. Experiment design and application

The experiments we performed are to some extent similar to those presented by Oke and England (2004) and Sijp and England (2008, 2009). Anomalies applied

TABLE 1. Sensitivity experiments and their integration periods (yr). IA: Interannual; REF: Reference; and SHW: Southern Hemisphere westerlies. Domain decompositions are depicted in Fig. 4.

Experiment	Domain	Description	Model configurations		
			ORCA05	AGIO	INALT01
IA	n/a	Interannual reference	1948–2007	—	1948–2007
REF	n/a	Climatological reference	1–110	1–60	1–60
SHW+4	FULL	4° equatorward shift	31–60	—	31–60
SHW+2	FULL	2° equatorward shift	31–60	—	—
SHW–2	FULL	2° poleward shift	31–60	—	31–60
SHW–4	FULL	4° poleward shift	31–60	—	—
SHW–40%	FULL	40% intensity decrease	31–110	31–60	31–60
SHW–40%	BASIN	40% intensity decrease	31–60	—	—
SHW–40%	LOCAL	40% intensity decrease	31–60	—	—
SHW–20%	FULL	20% intensity decrease	31–60	31–60	—
SHW+20%	FULL	20% intensity increase	31–60	31–60	—
SHW+40%	FULL	40% intensity increase	31–110	31–60	31–60
SHW+40%	BASIN	40% intensity increase	31–80	—	—
SHW+40%	LOCAL	40% intensity increase	31–80	—	31–60
SHW+40%	ACC-P	40% intensity increase	31–60	—	—
SHW+40%	ACC-B	40% intensity increase	31–60	—	—
SHW+40%	ACC-L	40% intensity increase	31–60	—	—
SHW+40%	ACC	40% intensity increase*	n/a	31–60	n/a

* AGIO boundary condition altered, further details in text.

to the present-day wind patterns (Fig. 3a) were designed to mimic different states in westerlies regime: equator- and poleward shifts of $\pm 2^\circ$ and $\pm 4^\circ$ of latitude (Fig. 3b) and intensity changes of $\pm 20\%$ and $\pm 40\%$ (Fig. 3c). The values chosen roughly span the range of observed (Swart and Fyfe 2012), twenty-first-century projected (Fyfe and Saenko 2006; Fyfe et al. 2007), as well as past (Hodgson and Sime 2010) changes in westerly winds. These anomalies have a smooth and quasi-sinusoidal shape to avoid any sharp changes or disruptions in the general wind stress curl pattern (that would alter the general pattern of the circulation). Additional design considerations were as follows: (i) Changes to the westerlies were limited to south of 35°S such that no changes are applied to the latitudes that would influence the inertia of the western boundary current; (ii) shifts were constructed based on the latitudinal location of the maximum wind stress and the total energy input kept constant; and (iii) the meridional wind stress components were unchanged. These considerations imposed limits to the extent the westerlies could be altered.

The resulting anomalies were reproduced onto the respective model grids. Out of the 8 anomalies (Figs. 3b,c), a total of 15 anomaly fields were produced (Table 1). For some anomalies, in particular the SHW+40% anomaly (westerlies intensity increase by 40%), in addition to changing the intensity of the wind stress, we altered the region over which these anomalies were applied (Fig. 4). These geographical decompositions attempt to determine the influence the Antarctic

Circumpolar Current may have on the Agulhas system. For these cases, additional smoothing was applied along the boundaries. The two-dimensional wind anomaly fields were added after calculation of the wind stress. Thus, the application influences the momentum and not the buoyancy input to the ocean–sea ice. This strategy follows Biastoch and Böning (2013), who performed a similar experiment within AG01.

All three models, sharing the same 20-yr spinup history, were forced under background CORE climatological forcing (Large and Yeager 2009). Figure 2 exemplifies the adjustment of the models. A relatively fast adjustment in volume-integrated kinetic energy to changes in resolution and forcing (application of anomaly) is noted. The reference experiments were integrated for 30 years before application of the anomalies. At first they were applied with a linear ramp up over one year (model year 31) and subsequently in full. Reference and sensitivity simulations ran parallel from model year 31. After two decades of parallel integration, analysis for all simulations was performed for a common period of 10 years (model years 51–60). The increasing kinetic energy after model year 45 in the global models for the SHW+40% examples shown in Fig. 2 reflects the transient response of the Agulhas system to the enhanced winds. This is discussed in section 4. Some selected experiments were extended, as outlined in Table 1. The global models were additionally integrated under interannually varying surface forcing, providing 6 decades (1948–2007) of hindcast simulations.

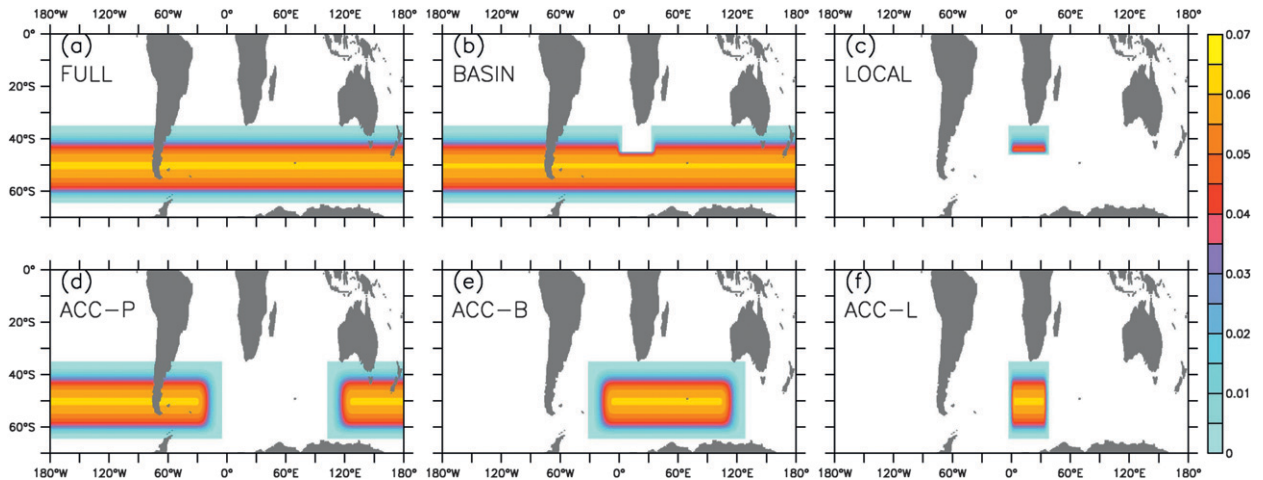


FIG. 4. Application of the SHW+40% anomaly (40% intensification of westerlies). The wind stress anomaly (N m^{-2}) is applied (a) circumpolarly (FULL); (b) circumpolarly except the region bounded by north of 45°S , 0° – 35°E (BASIN); (c) only over the region 35° – 45°S , 0° – 35°E (LOCAL); (d) over region west of 18°E and east of 115°E (ACC-P); (e) within region 18°W – 115°E (ACC-B); and (f) within region 0° – 35°E (ACC-L).

d. Model validations

Given the dominance of mesoscale variability, direct one-to-one comparison with features observed during oceanographic expeditions cannot be expected, even though a high-frequency, interannually varying forcing is used. However, time-mean properties and statistical representation of the variability ought to be comparable. ORCA05 is an established configuration of NEMO (Biaostoch et al. 2008a). Both AGIO and INALT01 are updates of previously thoroughly tested configurations: SAfE (Penven et al. 2006) and AG01 (Biaostoch et al. 2008b,c, 2009a; van Sebille et al. 2009, 2010), respectively. Within ORCA05, the Agulhas Current is represented by a continuous flow that begins in the northern Mozambique Channel with the only source of variability originating south of Madagascar. The current retroflects and occasionally produces some large unrealistic rings. In contrast, within AGIO and INALT01, where the first baroclinic Rossby radius of deformation is resolved (20–50 km in this region; Chelton et al. 1998), a broad spectrum of mesoscale activity is observed in the known source regions of the Agulhas Current as well as a more realistic representation of the diverse range of features typically found in the Cape Cauldron, namely Agulhas rings, cyclones and filaments among others (Boebel et al. 2003). Figure 5 portrays the model reproduction of the mean circulation as well as the mesoscale variability of the Agulhas system compared to that observed from satellite altimetry (Fig. 5a). The mean circulation is successfully represented by all three models; the details of the variability do however differ.

e. Assessing Agulhas leakage

Measuring Agulhas leakage is no simple task. Being highly intermittent, leakage occurs predominantly through Agulhas rings. However, other features such as cyclones and filaments also contribute to the Indian–Atlantic transport. Therefore, direct quantification of Agulhas rings crossing the Cape Basin would likely underestimate leakage magnitude (de Ruijter et al. 1999), while full-depth Eulerian measurements would over estimate it. Attempts at estimating leakage using optimized Eulerian methods have been made (van Sebille et al. 2010) but the skills of such methods have not been tested across models with different horizontal and vertical resolutions. From float and drifter observations, Richardson (2007) estimated leakage to be at about 15 Sv.

Here, we estimated annual values of leakage using a Lagrangian method following the works of Speich et al. (2001), Biaostoch et al. (2008b, 2009b), and van Sebille et al. (2009). Water parcels were released every 5 days for one year over the full depth of the poleward-flowing Agulhas Current across a zonal 300-km-long segment at 32°S . Each parcel had a defined transport of max. Here, 0.1 Sv and the total number of parcels released were representative of the 5-daily magnitude of the Agulhas Current. The parcels were then advected using the model's velocity fields for a total period of five years and aggregated across predefined sections. The integration period optimally allowed 98% of the parcels to exit the domain shown in Fig. 5d. Agulhas leakage is defined as that portion of the Agulhas Current exiting the domain through the Good Hope section (Ansong et al. 2005) in the Cape Basin (Fig. 5b). The advantage of

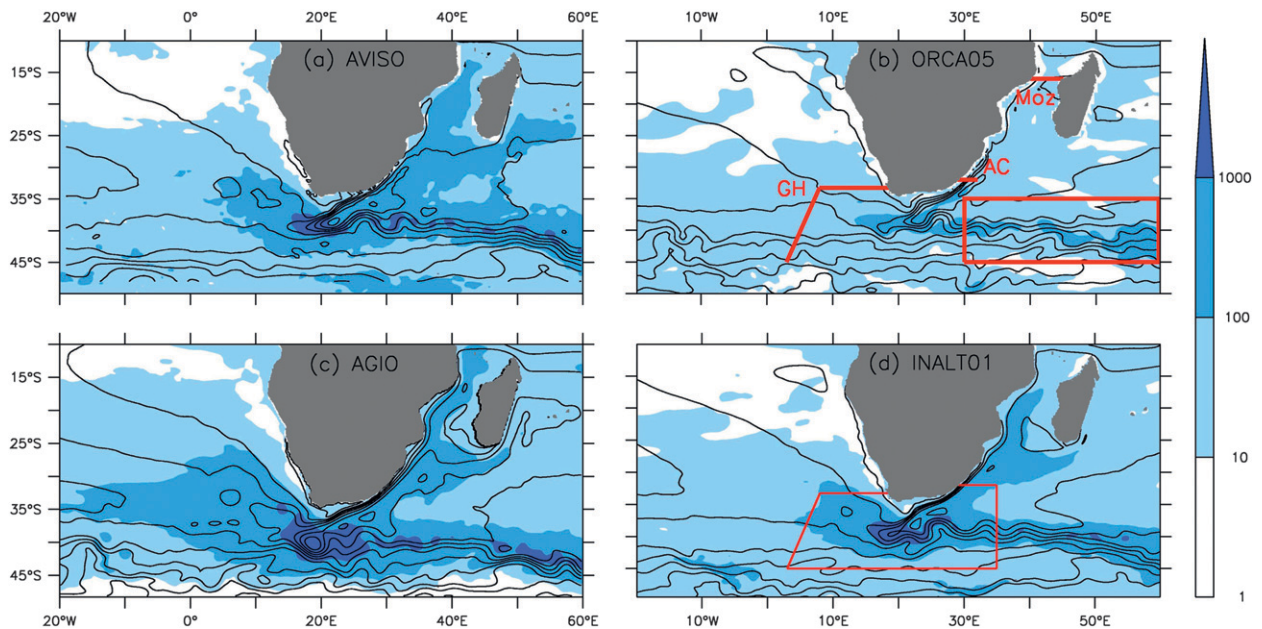


FIG. 5. Representation of mean circulation [contours of sea surface height (SSH) averaged for period 1992–2007] and mesoscale variability (shading of SSH variance; cm²) from (a) altimetric observation Archiving, Validation, and Interpretation of Satellite Oceanographic (AVISO) data, (b) ORCA05, (c) AGIO, and (d) INALT01. Sections used to measure Agulhas leakage across the Good Hope Line (GH), the AC, the Mozambique Throughflow (Moz), and the region where the Agulhas Return Current is monitored (box) are shown in (b). The domain used for the Lagrangian analysis is shown in (d).

this method is that it can be applied to all three models without the need for additional model-specific redefinitions, allowing direct intermodel comparisons. The southward transport of the Agulhas Current at 32°S for model years 51–60 of the three REF experiments are 71.9 ± 0.7 , 72.9 ± 3.1 and 64.6 ± 2.6 Sv for ORCA05, AGIO, and INALT01, respectively. The corresponding reference leakage values for the same period are 31.9 ± 1.5 , 31.5 ± 1.4 , and 16.6 ± 1.7 Sv, respectively. It is clear that leakage is markedly influenced by the regional mesoscale (Blastoch et al. 2008c).

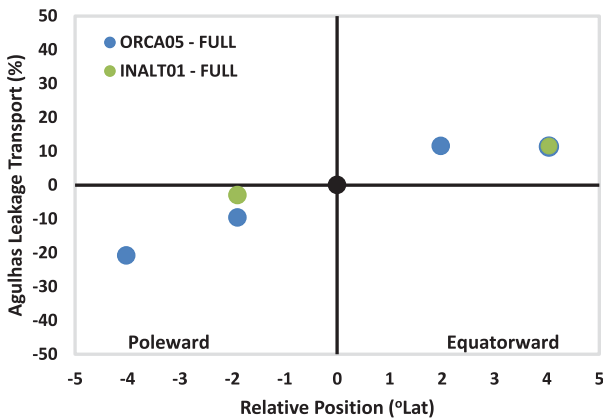
3. Agulhas leakage equilibrium response

Owing to the different reference values of Agulhas leakage in the three models, we adopt the percentage change with respect to reference as a measure of leakage response. This places all reference values at the origin. The 10-yr-mean (model years 51–60) leakage response to changes in position (Fig. 6a) and intensity (Fig. 6b) of the westerlies display three clear patterns. First, within the global models, an equatorward (poleward) shift in westerlies produces an increase (decrease) in leakage. Note that AGIO's southern boundary at 48°S makes shift experiments not sensible. Second, increasing intensity of westerlies generally produces more leakage but the relationship is not completely linear. Finally,

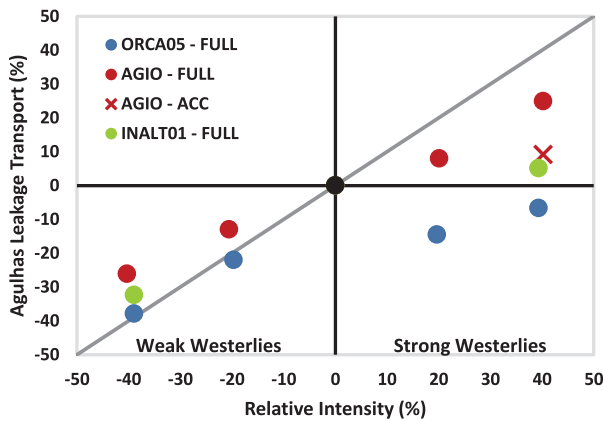
leakage responds preferentially, and the magnitude of that response is more pronounced when changes are applied to the intensity of westerlies than shifts. For this reason, we will concentrate on the intensity cases and return to the shifts toward the end. Interestingly, for strong wind stress in Fig. 6b, both global models simulate very little leakage change and even reduction compared to the reference values. Conversely, a 20% and 40% reduction in wind stress produces approximately the same amount of leakage decrease. Consistent with Le Bars et al. (2012), there appears to be a threshold in leakage response to increased westerlies.

To investigate the reason for this threshold, we focus on two extreme intensity cases, $\text{SHW} \pm 40\%$ within ORCA05. The Agulhas system, forming part of the subtropical gyres of the South Atlantic and South Indian Oceans (Ridgway and Dunn 2007) and bounded by the Antarctic Circumpolar Current, potentially could be influenced by numerous external factors. In an attempt to therefore distinguish between local and large-scale wind impact on leakage, a geographical decomposition of the $\text{SHW} \pm 40\%$ experiments was performed (Figs. 4a–c). We favored the use of the coarse-resolution ORCA05 model because it is computationally less demanding. The response shown in Fig. 6c reveals that the overall leakage response consists of the direct influence of the westerlies acting locally (over the Agulhas retroflection

(a) SHW - Position



(b) SHW - Intensity



(c) SHW - Intensity Decomposition

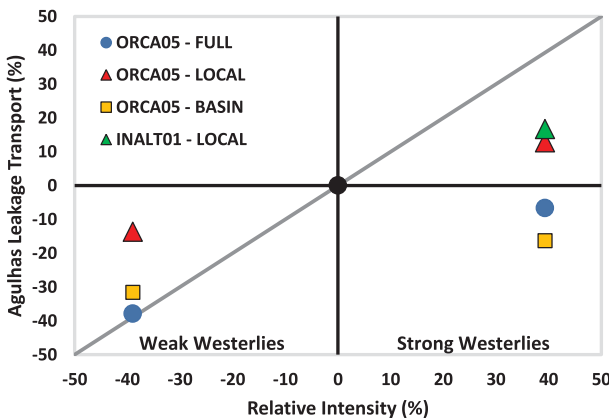


FIG. 6. Change in Agulhas leakage (%) vs change in (a) position ($^{\circ}$ lat) and (b),(c) intensity (%) of SHW. Reference values (black dot) are set at the origin for all three models and each dot represents a decade average (model years 51–60; blue shading in Fig. 2). The decomposition between FULL, BASIN, and LOCAL is shown for the SHW–40% and SHW+40% cases in (c). The gray lines in (b),(c) represent the theoretical change in Sverdrup transport.

and Cape Basin region) on the magnitude of the leakage and on the indirect influence of the winds via the adjacent currents. INALT01, the configuration that mimics the known complexity of the Agulhas system with the highest degree of semblance, reproduces the general behavior in leakage. Leakage response within INALT01–SHW+40% with LOCAL decomposition shows that, despite the overestimation of absolute leakage values within the coarse-resolution model, the change in leakage is consistent. The decompositions further indicate that the threshold in leakage change originates from the large-scale circulation, within which the Agulhas system is embedded.

This hypothesis is tested by employing the regional model, AGIO, whose domain excludes much of the large-scale circulation (Loveday et al. 2013, manuscript submitted to *J. Phys. Oceanogr.*). The global ocean influences this regional model through lateral boundary conditions derived from climatology of the ORCA05–REF simulation. Here, leakage response is quasi linear, monotonously increasing with strengthening westerlies (Fig. 6b). This suggests that, with a constant climatological representation of large-scale circulation, in particular that of the Southern Ocean, the portion of the westerlies felt within AGIO’s southern domain (35° – 48° S) does not cause a threshold in leakage response. Altering the boundary conditions to that derived from the ORCA05–SHW+40% experiment (red cross in Fig. 6b), effectively allows for an assessment of the influence a different Southern Ocean state has on leakage. In this case, leakage behavior is similar to that of the two global models, supporting the hypothesis that the threshold observed in leakage (Fig. 6b) originates from the large-scale circulation.

4. Agulhas leakage transient response to increased westerlies

For the purpose of exploring the time dependency of Agulhas leakage response to increased westerlies, we focus on the SHW+40% case and expand the ORCA05 simulations to beyond the 10 years of common analysis. Figure 7 shows the time evolution of leakage and other parameters associated with the greater Agulhas system. Presented are the annual values beginning from model year 31, which is when the anomaly fields are applied. Linear trends calculated from the reference experiment were removed from all runs. Under background climatological forcing, these minor trends (between 0.1% and 2.5% decade $^{-1}$ of the reference values) represent the inherent numerical drift that can reasonably be assumed to be similar in all simulations. The BASIN and LOCAL decompositions are overlaid. Following a fast initial adjustment, three distinct stages in leakage behavior in

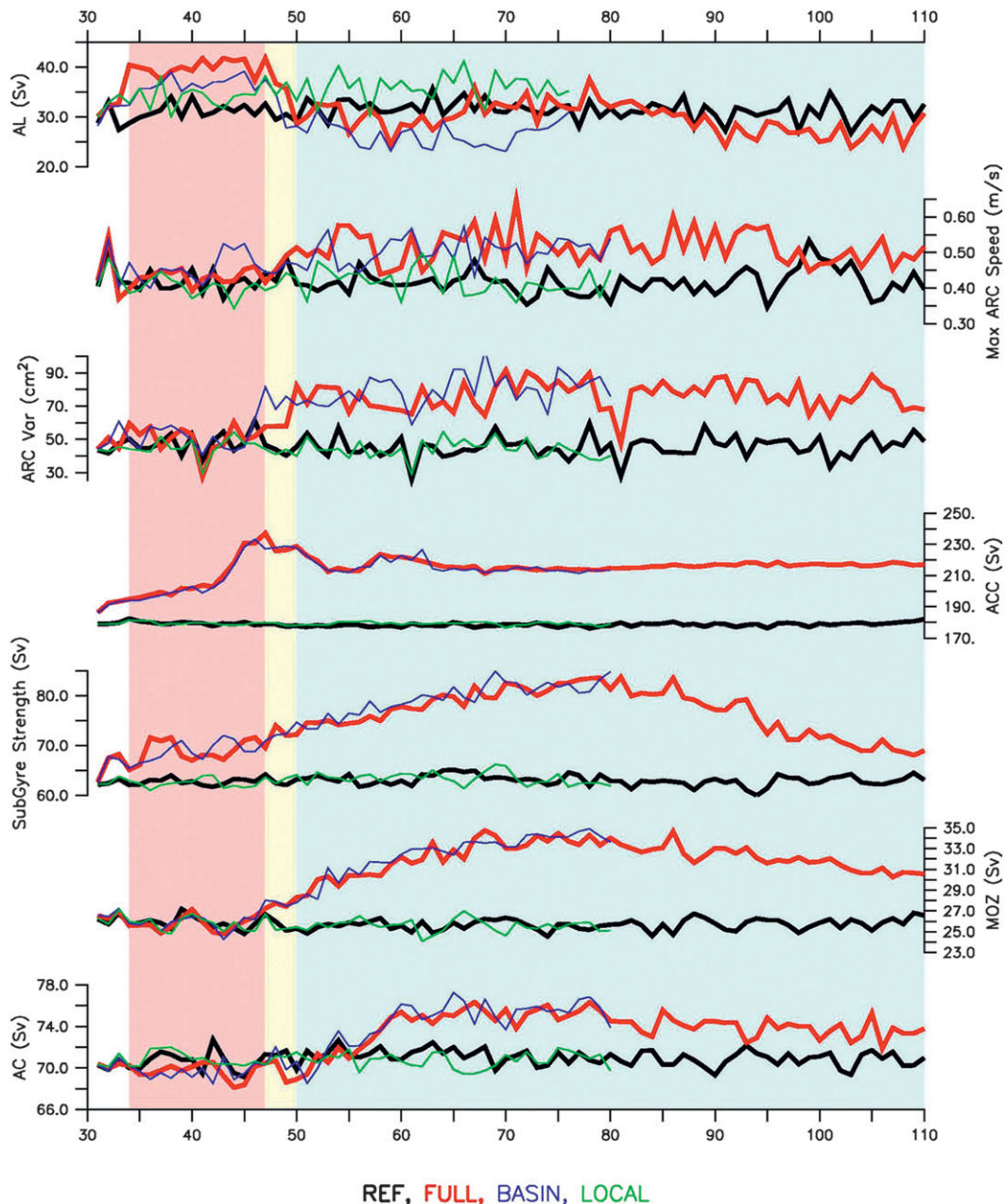


FIG. 7. Time series for the REF and SHW+40% cases within ORCA05. Sections used to measure the transports are shown in Fig. 5a and aside from the AL, all transports are measured from the barotropic streamfunction: the ACC as the maximum streamfunction south of Africa between 20° and 30° E; the subgyre strength as the min streamfunction value between 30° and 60° E; and the AC as the min streamfunction along the section at 32° S. For the ARC, speed is for the top 1000 m. The light red, yellow, and blue shadings indicate Stage 1, Stage 2, and Stage 3 in ORCA05–SHW+40%–FULL leakage response, respectively (details in text).

the ORCA05–SHW+40%–FULL case (red curve on Fig. 7) can be noted: (i) A proportional increase (model year 34–47) followed by (ii) a rapid decline (model year 47–50), and finally (iii) return to and decadal modulation around reference values (beyond model year 50).

Stage 1: Lasting for about a decade, the westerlies acting both locally and outside the Agulhas region contribute toward increasing the leakage. This produces an overall proportional response (40% increase in winds resulting in $\sim 40\%$ increase in leakage), with a 1:3 ratio

between LOCAL and BASIN. During Stage 1, the mean value of leakage for the FULL experiment is significantly different at the 99% confidence level (Welch's t test) from the mean leakage value of the reference experiment. As anticipated, no change is observed in the Agulhas Current, the Agulhas Return Current (ARC), and Mozambique Throughflow, because surface forcing is unchanged equatorward of 35°S. The ACC and southwest Indian subgyre, during that period, adjust to the altered forcing, which thereafter determines the time scale of the leakage response. Note that we opt to measure the barotropic ACC transport south of the African continent, the region that is most likely to impact the Agulhas system. Qualitatively, there is little difference from measuring at other choke points, at Drake Passage for example, where the reference value of ACC transport is about 130 Sv, falling within observed ranges (Meredith et al. 2011).

Stage 2: Happening rapidly, within four model years (47–50), the decline appears to occur indirectly as a result of the large-scale circulation adjustment. Without the large-scale adjustment, a local increase in westerlies would maintain an increased leakage. The decline coincides with the peak in ACC, the increase in ARC transport and variability, and the increase in Mozambique Throughflow. The Agulhas Current also begins to respond accordingly.

Stage 3: Approximately two decades after the initial anomaly application, leakage falls within the variability range of the reference experiment (with some decadal variations around it). For Stage 3, the mean leakage value of the FULL experiment is significantly not different at the 99% confidence level from the reference value. In response to a 40% increase in westerlies, the ACC stabilizes to $\sim 20\%$ above reference (Fig. 7). A strengthened subgyre is noted in addition to an increase in Mozambique Channel flow (by $\sim 25\%$) and subsequent downstream increase of the Agulhas Current (by $\sim 5\%$). This Agulhas Current transport increase occurs as an indirect effect of the westerlies increase. No change in the East Madagascar Current transport is noted (not shown). The ARC speed remains at an increased level ($\sim 23\%$ above reference values), with a $\sim 60\%$ increase in variance. Toward the end of the simulation (model year 90 onward), because of the increased wind stress curl acting only over the southern portion of the subtropical gyres, the stronger subgyre meridionally contracts and zonally widens. This is subsequently seen in a slight reduction in Mozambique Throughflow and Agulhas Current transport. The return of leakage to reference values occurs because of the large-scale circulation, as suggested by the BASIN experiment.

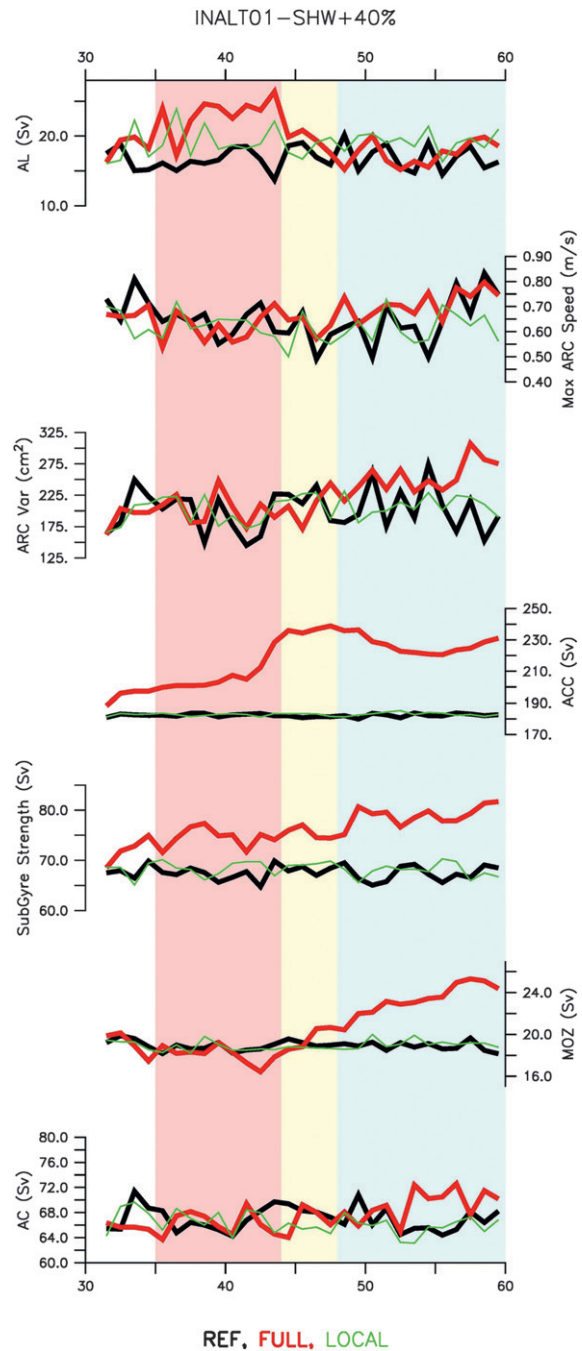


FIG. 8. As in Fig. 7, but for INALT01.

Figure 8 shows the equivalent within INALT01. Comparing the two global models provides a way of diagnosing the impact mesoscale activities of the wider Agulhas region have on the leakage response. Perhaps surprisingly so, but as already seen in Fig. 6, the general response to westerly winds increase is not altered. The adjustment happens quicker, and Stage 3 is reached 2–3 years earlier. To test the impact of resolution on domain

decomposition, the LOCAL experiment (only decomposition falling entirely within INALT01's nest boundaries) was repeated within INALT01. The response is similar to what was anticipated (Figs. 6b and 8). The fact that the models agree in the response, irrespective of resolution, points toward an underlying mechanism that is to some extent resolution independent.

The response seems to be linked to the development of the ACC. In the Atlantic sector of the Southern Ocean, an increase in westerlies promotes a spinup of the Weddell Gyre and, because of an increased pressure gradient, also its expansion (not shown). This in turn leads to an overall increase in the width of the circumpolar current in the Atlantic. Within the two global models, the dynamic front between the supergyre and the ACC regime can be diagnosed from the zero barotropic streamfunction line (see Fig. 3a). During Stage 3, immediately south of the leakage corridor, this boundary migrates by $\sim 2^\circ$ equatorward.

In the Southern Ocean, resolving eddies is known to be important (Hallberg and Gnanadesikan 2006; Böning et al. 2008; Spence et al. 2010). The ACC within INALT01 is represented at the same resolution as within ORCA05. Owing to the two-way nesting scheme adopted for INALT01 and the requirement for consistent comparisons across models, the choice has been made not to parameterize eddies in ORCA05. However, in order to assess the dependence of the three-stage response on first Southern Ocean eddies and second initial conditions, we repeated the ORCA05-REF and ORCA05-SHW+40%-FULL experiments including the initial 20-yr spinup with parameterized eddies (Gent and McWilliams 1990). Thickness diffusivities used are capped at $1000 \text{ m}^2 \text{ s}^{-1}$ but vary spatially and temporally, increasing with stratification and isopycnal slope. These simulations showed the same three-stage behavior in leakage response (including the magnitude of the Stage-1 increase), with the only difference being a prolonged Stage 2 (figure not shown).

Seeking to confirm that the ACC generally influences Agulhas leakage, three additional experiments were undertaken. In these experiments, the SHW+40% anomaly field was further decomposed geographically and applied within ORCA05 (Figs. 4d-f). Figure 9 shows the general behavior in ACC-B and ACC-L following the same three-stage pattern as for FULL (Fig. 7). Within the given time frame, no response is seen when the ACC-P decomposition is applied, potentially indicating that the westerlies acting over the Pacific Ocean, Drake Passage, and south of Australia, under this setup, have no direct immediate impact on leakage. A possible reason for this would be that the westerlies, generally weaker in strength and lying about 5° poleward in the

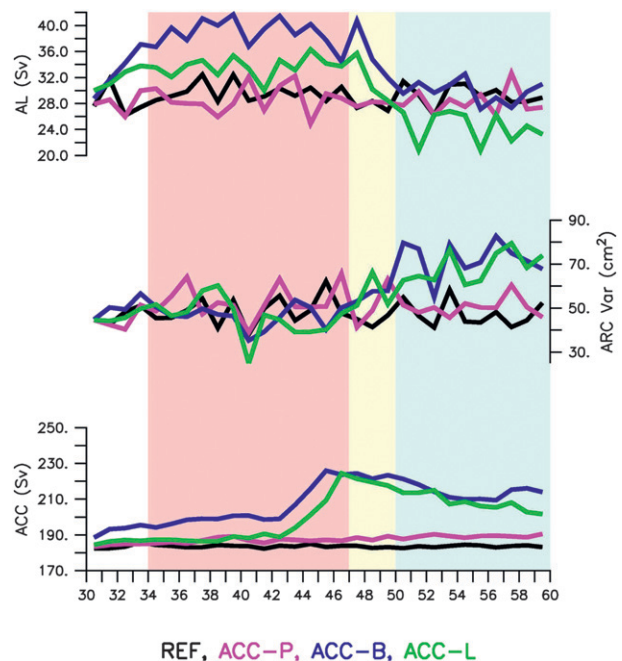


FIG. 9. Time series of AL, ARC variance (ARC Var), and ACC transport from the ACC-P (pink), ACC-B (blue), and ACC-L (green) decompositions of the SHW+40% anomaly within ORCA05. The light red, yellow, and blue shadings indicate Stage 1, Stage 2, and Stage 3 in ORCA05-SHW+40%-FULL leakage response, respectively (extracted from Fig. 7).

Pacific compared to the Indian-Atlantic sector (Fig. 3), are not aligned to the core of the applied anomaly. The response in ACC-B, similar in magnitude to that of FULL, suggests that the winds in the region 18°W - 115°E , corresponding to the region of maximum climatological westerlies (Fig. 3), set the leakage response. Further confirming the ACC's influence, ACC-L, a poleward extension of the LOCAL application, shows an initial increase of the same magnitude as LOCAL and a subsequent three-stage leakage response.

The time scale is set by the ACC. Following the ACC peak, both the leakage and ARC (transport and variance) react with a decline and an increase, respectively (Figs. 7-9). Averaging over two 5-yr periods reveals that, in Stage 1, the leakage increase is coincidental with an increased eddy kinetic energy in the Cape Basin, but with a decrease in the retroreflection region (Figs. 10a,c). Flowing adjoined and unidirectional to each other, the interaction between the ACC and the ARC become important in Stage 3, where both the retroreflection and the ARC become more energetic and variable (Figs. 7-9; Figs. 10b,d). This is characteristic of a turbulent retroreflection regime (Le Bars et al. 2012). This regime, which occurs at strong winds, leads to the increased volume transport (seen in Stage 1 as increased leakage) to be

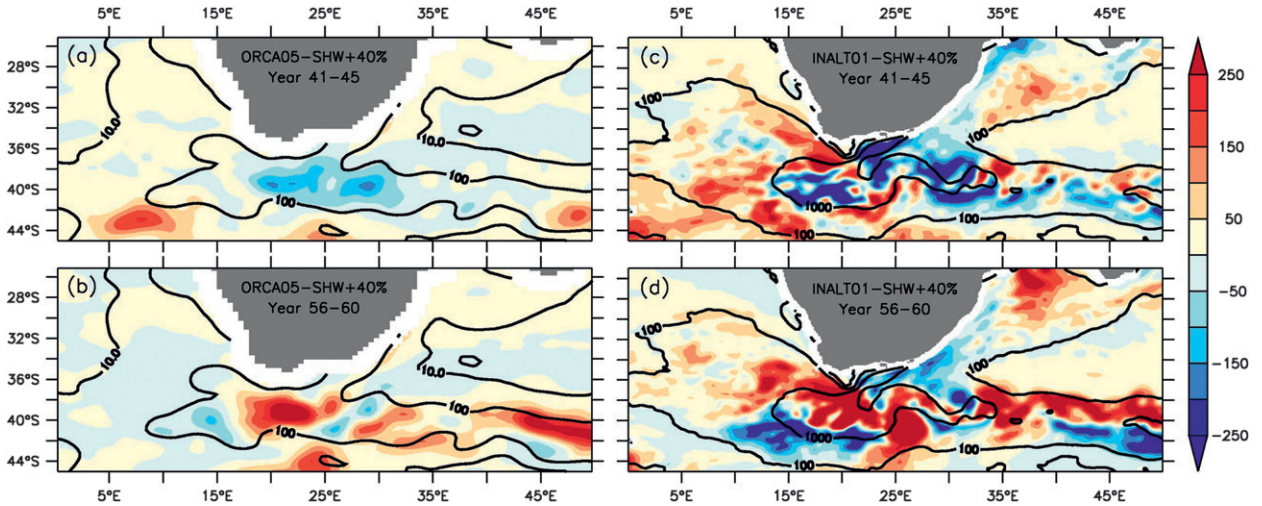


FIG. 10. EKE per unit mass anomaly at 100 m ($\text{cm}^2 \text{s}^{-2}$) within (a),(b) ORCA05 and (c),(d) INALT01 averaged over model years 41–45 (top) and 56–60 (bottom). Contours indicate the respective averaged reference EKE values for model years 41–60.

lost through an enhanced interaction between the ARC and the ACC.

5. Mechanism of leakage response to the westerlies

The region of positive wind stress curl in the South Indian and South Atlantic Oceans roughly lies between 15° (maximum trades) and 50°S (maximum westerlies). The wind stress curl yields negative Ekman vertical velocities (i.e., pumping) over this region, which promotes an equatorward Sverdrup transport of the interior (Marshall and Plumb 2007). Figure 11 schematically portrays the proposed mechanism of leakage response to changes in the westerlies. Increasing the westerlies in the manner presented in this study leads to an increased wind stress curl between the latitudes 35° and 50°S. The equatorward interior flow across the southern portion of the

supergyre is therefore enhanced. In Fig. 11, this is depicted along 40°S, which roughly is the latitude of separation between the westward-flowing Agulhas leakage and the eastward-flowing Agulhas Return Current. By construction no change is applied to the winds at the latitudes of the Agulhas Current, north of 35°S. Through continuity, the increased meridional transport must result in a westward mass transport toward South America. Closing the circulation, the western boundary current subsequently increases.

Figures 6b and 6c (gray lines) also show the change in theoretical meridional interior flow (Sverdrup transport) along 40°S resulting from the added intensity anomalies. As anticipated, the change in Sverdrup transport is a linear function of the change in wind stress curl. Our results show that leakage change within the global models follows the proportional Sverdrup transport change over the entire

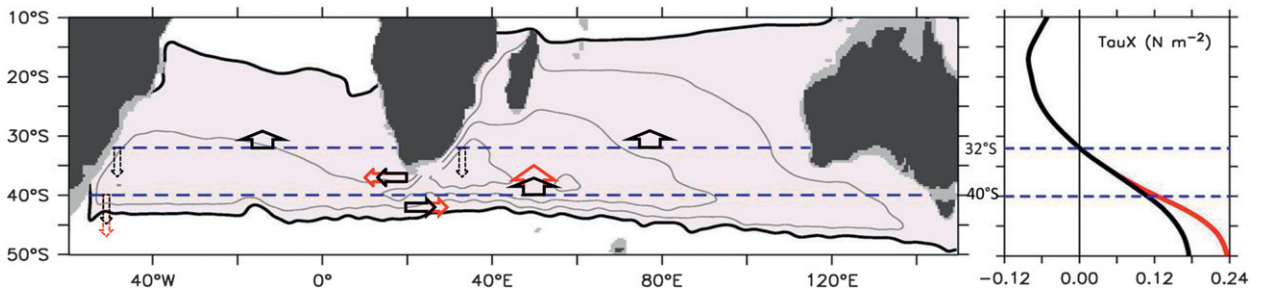


FIG. 11. Schematic of the proposed mechanism of leakage response to the westerlies. Contours of barotropic streamfunction portray the anticyclonic supergyre (shaded area) connecting the South Indian and South Atlantic Oceans, with a thick black contour demarcating its boundaries (data extracted from ORCA05–REF experiment). Thick arrows indicate the meridional Sverdrup interior flow and the corresponding zonal transport that results from the wind stress application (REF in black and SHW+40% in red; associated wind stress pattern shown in the right panel). The circulation is closed by the return flow of the western boundary currents (dotted arrows).

time series for the reduced westerlies cases (Fig. 6b) and during Stage 1 of the intensified westerlies simulations (Figs. 7 and 8).

In the portrayal shown in Fig. 11, leakage corresponds to the westward flow south of the African continent and is a passive component of the supergyre circulation. This has three major implications. First, it suggests that the process determining leakage would be independent of retroflection energetics. In partial support for this, we showed that eddy kinetic energy of the retroflection in Fig. 10 matches in sign with neither the initial increase in leakage of Stage 1 nor the return to reference values in Stage 3. Eddy kinetic energy of the retroflection is increased in Stage 3 compared to reference levels, while leakage is unchanged. Therefore, there seems to be no link between the energetics of the retroflection and the process behind leakage. Second, it backs up the conclusion of Loveday et al. (2013, manuscript submitted to *J. Phys. Oceanogr.*), who showed leakage to be decoupled from changes in the Agulhas Current. During Stage 1, a large response in leakage occurs without any change in Agulhas Current. In Stage 3, the increase in Agulhas Current (an indirect consequence of the westerlies increase) results in no change in leakage. Third, as noted in Figs. 6–8, the general pattern of leakage response to the change in westerlies is reflected at all resolutions; in other words, irrespective of the form of leakage. It is important to mention here that we do not claim that leakage follows Sverdrup dynamics because nonlinearity plays a crucial role in determining the amount of water entering the South Atlantic. What we noticed is that, given a change in the westerlies, leakage responds in the same way the interior adjustment (described by the Sverdrup balance) does.

Agulhas leakage response is transient (Figs. 7–9). The time dependency is a question of wave propagation, in particular internal planetary waves, similar to the process that communicates the dynamical imprint of leakage across the South Atlantic (van Sebille and van Leeuwen 2007; Biastoch et al. 2008b). Rossby waves set the adjustment time of the ocean to large-scale forcing. The initial rapid oceanic adjustment to the applied high-frequency wind forcing prior to Stage 1 (model years 31–33) is a result of the fast propagation of barotropic Rossby waves, which establishes the Sverdrup balance. Meanwhile, the influence of westerly winds induces a baroclinic adjustment of the eastward-flowing ACC on decadal time scale. Additional controls, such as its width, its variability, and buoyant convection within and outside of the current further influence the adjustment time scale of the ACC (Allison et al. 2011). The timing in Figs. 7–9 suggests that the interaction between the ACC and the Agulhas system becomes important after

1–2 decades. The decrease in leakage in Stage 3 is preceded by an increasing variability of the ARC, which occurs when the ACC reaches its peak. The precise mechanism behind this interaction is beyond the scope of this study. Because both currents are unidirectional and adjacent, meridional exchanges in lateral momentum and tracers between them may be a likely explanation.

Thus far, we focused on the impact of the intensity of westerlies on the Agulhas system. As noted earlier, idealized equatorward shifts of the westerly wind belt induces an increase in leakage (Fig. 6a). This occurs as a result of the redistribution of momentum. Our application of a northward shift of the westerlies strengthens the wind stress curl between 35° and 45°S, while reducing it over the core of ACC (45°–60°S). The overall effect is similar to an increase in westerlies over the southern portion of the Indian Ocean subtropical gyre that leads to an increase in leakage. In this case, leakage remains at a constant increased level (persistent Stage 1) and a weaker ACC does not result in leakage to be hampered. The opposite for poleward shifts also holds; reduced northward Sverdrup transport across the southern boundary of the supergyre boundary leads to reduced leakage. Toward the end of the SHW–4 simulation, there is an indication that the leakage further decreases, exacerbated by an increased ACC that stimulates an enhanced interaction with the retroflection and ARC. This, once again, is dynamically consistent, as described above.

6. Discussion

There is the common belief that a displacement of the zero wind stress curl line equatorward (poleward) would narrow (widen) the gateway south of Africa allowing less (more) leakage (Zahn et al. 2010). Our result shows the converse. Paleoceanographic interpretations propose that, on centennial–millennial time scales, a displacement of the subtropical front at the northern boundary of the ACC south of Africa, concomitant with shifts and intensity changes in the westerlies, could be a major driver in modulating the amount of leakage (Peeters et al. 2004; Bard and Rickaby 2009; Caley et al. 2012). In our series of experiments, we observed no significant change in the latitudinal position of the hydrographically defined subtropical front (maximum temperature gradient) south of Africa in response to changes in position of the zero wind stress curl line. However, we cannot emphatically conclude that the front does not respond to westerly changes, because we did not apply a corresponding thermohaline forcing. Our ocean/sea ice–only simulations addressed the transient response of the Agulhas system. Processes such as deep and bottom water formation, which

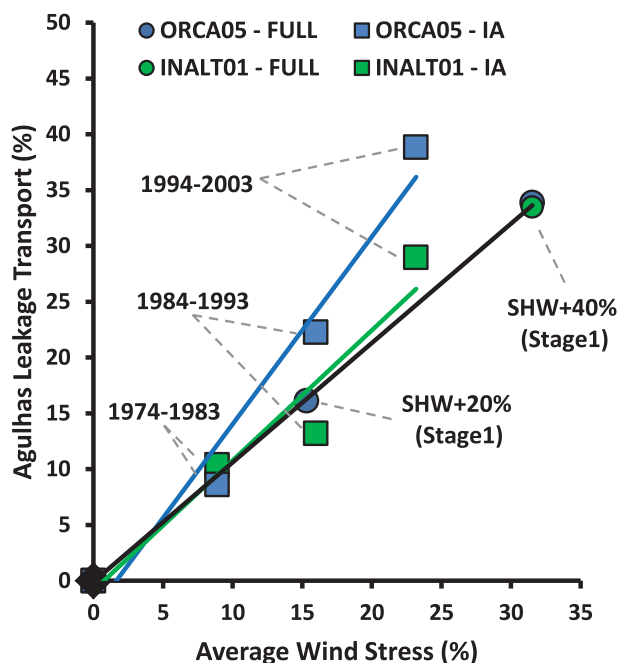


FIG. 12. Change in Agulhas leakage (%) vs change in wind stress (%) averaged over the region 35° – 65° S, 20° W– 140° E. Squares represent decadal averages from hindcast IA simulations of ORCA05–IA (light blue) and INALT01–IA (light green), with the period 1964–73 taken as reference (set at origin). Circles represent Stage-1 averages (model years 41–45) from the FULL application of the SHW+20% and SHW+40% anomalies as well as the corresponding REF (set at origin) within ORCA05 (blue) and INALT01 (green).

indirectly respond to changing wind patterns, would in the long term affect the hydrography of the Southern Ocean leading to possible shifts of its fronts (Spence et al. 2010; Downes et al. 2011; Graham et al. 2012).

During the Last Glacial Maximum ($\sim 20\,000$ years ago), leakage reduction (Peeters et al. 2004; Franzese et al. 2006) and possible ACC increase (Franzese et al. 2006; Otto-Bliesner et al. 2006) with no change in retroflexion position (Franzese et al. 2009) have been suggested. There is, however, large uncertainty regarding the state of the Southern Hemisphere winds during glacial times (Kohfeld et al. 2013). To name but a few examples of recent studies, Anderson et al. (2002) and Wyrwoll et al. (2000) reported an intensifying poleward displacement of the westerly jet; Rojas et al. (2008) concluded a decrease with no significant latitudinal shift while Toggweiler et al. (2006) deduced an equatorward shift. It is therefore not possible, given the present limited knowledge of the wind patterns of the Last Glacial Maximum, to confirm whether the dependency of Agulhas leakage on the westerlies was dominant. Nonetheless, a leakage reduction accompanied by a more vigorous ACC would be in line with our results.

Of current relevance, models simulate an increase in contemporary Agulhas leakage (Biastoch et al. 2009a; Rouault et al. 2009). Biastoch et al. (2009a) proposed that a poleward shift in contemporary westerlies is responsible for this increase. Swart and Fyfe (2012) questioned the robustness of such a latitudinal shift in present-day westerlies in an analysis of various coupled climate model products as well as observational reanalysis and found that instead of a shift, significant strengthening of the westerlies has occurred. In the last 40 years, the westerlies have increased by about 25% (Fig. 12). We showed that leakage initially responds proportionally to increased westerlies (Stage 1 in Figs. 7 and 8). In Fig. 12, this is reflected by the linear relationship for the SHW+20% and SHW+40% cases. Note that Fig. 12 shows the area-averaged (35° – 65° S, 20° W– 140° E) change in westerlies and not the change in maximum zonal-averaged westerlies. Also shown are decadal averages in leakage change derived from the hindcast experiments of ORCA05 and INALT01. Given the strong linear relationship ($r = 0.98$ and 0.96 for ORCA05 and INALT01, respectively), similar to that of the sensitivity experiments, we can conclude that the upward trend in leakage reported by Biastoch et al. (2009a) and Rouault et al. (2009) may reflect an unadjusted oceanic response to the continuously increasing momentum input by the westerlies akin to Stage 1. We could further speculate that, should the ongoing wind change lessen or halt (Watson et al. 2012) in response to stratospheric ozone recovery (Son et al. 2010), future decadal trends in leakage could weaken. This would naturally also depend on the timing and magnitude of the ACC response. It is unclear whether the ACC is already eddy saturated (Hallberg and Gnanadesikan 2006; Böning et al. 2008; Spence et al. 2010). We have shown that the circumpolar current plays a relatively critical role in the transient three-stage leakage response. Therefore, should the ACC be weakly responsive (or unresponsive) to the present-day increasing westerlies, a delay in the onset of a Stage 2-type leakage response can be expected.

Rouault et al. (2009) and van Sebille et al. (2009) both related the strength of the Agulhas Current with the magnitude of leakage. Within the present-day range of transport values, they found a linear relationship between the two variables. They did, however, disagree on the sign of that relationship. Results presented here suggest that changes in leakage do not necessitate variations in upstream transport. The Agulhas Current is influenced by both easterlies (Loveday et al. 2013, manuscript submitted to *J. Phys. Oceanogr.*) and westerlies (this study, Stage 3), while leakage responds predominantly to the westerlies. The disagreement between Rouault

et al. (2009) and van Sebille et al. (2009) was most likely an outcome of the different wind field products used in forcing their respective models. In general, within an integral large-scale atmospheric system, statistical relationships between the Agulhas Current and leakage do not necessarily imply cause and impact but instead are manifestations of individual external forcing.

Resolution is an important aspect of Agulhas system modeling. The necessity to resolve the Agulhas system adequately has been amply emphasized in the literature (e.g., Biastoch and Krauss 1999; Biastoch et al. 2008c). Beal et al. (2011) even recommend that at least a tenth-degree horizontal resolution (e.g., INALT01) is required. Such resolution has not yet been reached by most coupled climate models used for future predictions (Taylor et al. 2012; Weijer et al. 2012). Here, while our series of experiments demonstrate that leakage response to a constant change in westerly winds is represented at all resolutions, we wish to stress the importance in considering the magnitude of the response. For example, a 40% increase in westerlies during Stage 1 results in approximately the same percentage increase in leakage, which at low resolution (ORCA05) is ~ 10 Sv and at high resolution (INALT01) is ~ 6 Sv. Coarse-resolution models clearly overestimate the actual volumetric transport and corresponding amount of heat and salt exported into the Atlantic, which ultimately is of critical importance because of the implications for the Atlantic meridional overturning circulation and global climate (Biastoch et al. 2008b,c). Notwithstanding, within the 0.5° – 0.1° range, the mechanism behind the response of leakage to changes in the westerlies is consistent.

Our study describes leakage response in the context of changes in the zonal component of westerlies that are constant in time. In reality, the wind system changes progressively and leakage is expected to respond nonlinearly to the compounding effects of migrations and magnitudes (deviation from linearity seen in Fig. 12). The meridional component of the wind stress, albeit relatively small on average, may additionally play a role that we have not considered here. Furthermore, changes in the transition zone between the easterlies and westerlies (between 25° and 35° S) as well as the impact of altered wind forcing on the thermohaline field may also be important.

7. Summary

We systematically deconstructed the manner in which the Southern Hemisphere westerlies affect Agulhas leakage and reached the conclusion that the intensity of the wind belt is predominantly responsible in controlling

the Indian–Atlantic transport. Agulhas leakage responds rapidly (within 2–3 years) and proportionally to changes in the westerly wind stress. Change in leakage is comparable to the change in Sverdrup transport across the southern portion of the supergyre. Shifts and modifications to the intensity of the wind belt result in changes in wind energy input that, following Sverdrup dynamics, cause an adjustment of the interior flow. South of Africa, that change is in turn reflected as a change of leakage.

Simulations where the intensity of the westerlies was increased show a transient response in leakage. Initially, leakage responds proportionally to the wind increase. Subsequently, after 1–2 decades, leakage subsides to normal reference levels. The transient response occurs because of the adjustment of the large-scale circulation. In particular, energetic interactions between the Antarctic Circumpolar Current and the Agulhas system cause the subsidence in leakage.

We also showed that the impact of a displacement of the westerly wind belt on leakage can be regarded as a redistribution of momentum. Shifts of the westerlies equatorward increase the energy input over the southern portion of the supergyre and reduce it over the Southern Ocean. This results in enhanced leakage. Conversely, poleward shifts reduce leakage and the reduction would be accentuated following the adjustment (strengthening) of the circumpolar current. This result is at odds with previous claims.

Our investigation further suggested that the process behind the leakage response to changes in the westerlies is independent of model resolution, upstream transport of the Agulhas Current, and possibly retroreflection energetics. However, this does not discredit the importance of nonlinearity in the region. The volumetric change in leakage within models is highly dependent on the correct representation of the numerous nonlinear interactions in the Agulhas system. More importantly, the corresponding changes in the amount of heat and salt being exported have the potential of impacting the circulation in the Atlantic.

Acknowledgments. This work received funding from the European Community's Seventh Framework Programme FP7/2007-2013-Marie-Curie ITN, under Grant Agreement 238512, GATEWAYS project. Model experiments were performed at the high performance computing centers in Stuttgart (HLRS) and in Cape Town (CHPC) as well as at the Christian-Albrechts-Universität zu Kiel (NESH). The Ariane-v2.2.6 Lagrangian package was used for Agulhas leakage calculation (<http://www.univ-brest.fr/lpo/ariane/>). Altimetry data for model validation were downloaded (<http://aviso.oceanobs.com>).

REFERENCES

- Allison, L. C., H. L. Johnson, and D. P. Marshall, 2011: Spin-up and adjustment of the Antarctic Circumpolar Current and global pycnocline. *J. Mar. Res.*, **69**, 167–189, doi:10.1357/002224011798765330.
- Anderson, R. F., Z. Chase, M. Q. Fleisher, and J. Sachs, 2002: The Southern Ocean's biological pump during the Last Glacial Maximum. *Deep-Sea Res. II*, **49**, 1909–1938, doi:10.1016/S0967-0645(02)00018-8.
- Ansorge, I., S. Speich, J. R. E. Lutjeharms, G. J. Goni, C. J. de W. Rautenbach, P. Froneman, M. Rouault, and S. L. Garzoli, 2005: Monitoring the oceanic flow between Africa and Antarctica: Report of the first Good Hope cruise. *S. Afr. J. Sci.*, **101**, 29–35.
- Arakawa, A., and Y.-J. G. Hsu, 1990: Energy conserving and potential-entrrophy dissipating schemes for the shallow water equations. *Mon. Wea. Rev.*, **118**, 1960–1969.
- Bard, E., and R. E. M. Rickaby, 2009: Migration of the subtropical front as a modulator of glacial climate. *Nature*, **460**, 380–383, doi:10.1038/nature08189.
- Barnier, B., and Coauthors, 2006: Impact of partial steps and momentum advection schemes in a global ocean circulation model at eddy-permitting resolution. *Ocean Dyn.*, **56**, 543–567, doi:10.1007/s10236-006-0082-1.
- Beal, L. M., and Coauthors, 2011: On the role of the Agulhas system in ocean circulation and climate. *Nature*, **472**, 429–436, doi:10.1038/nature09983.
- Biastoch, A., and W. Krauss, 1999: The role of mesoscale eddies in the source regions of the Agulhas Current. *J. Phys. Oceanogr.*, **29**, 2303–2317.
- , and C. W. Böning, 2013: Anthropogenic impact on Agulhas leakage. *Geophys. Res. Lett.*, **40**, 1138–1143, doi:10.1002/grl.50243.
- , —, J. Getzlaff, J.-M. Molines, and G. Madec, 2008a: Causes of interannual–decadal variability in the meridional overturning circulation of the midlatitude North Atlantic Ocean. *J. Climate*, **21**, 6599–6615.
- , —, and J. R. E. Lutjeharms, 2008b: Agulhas leakage dynamics affects decadal variability in Atlantic overturning circulation. *Nature*, **456**, 489–492, doi:10.1038/nature07426.
- , J. R. E. Lutjeharms, C. W. Böning, and M. Scheinert, 2008c: Mesoscale perturbations control inter-ocean exchange south of Africa. *Geophys. Res. Lett.*, **35**, L20602, doi:10.1029/2008GL035132.
- , L. M. Beal, J. R. E. Lutjeharms, and T. G. D. Casal, 2009a: Variability and coherence of the Agulhas Undercurrent in a high-resolution ocean general circulation model. *J. Phys. Oceanogr.*, **39**, 2417–2435.
- , C. W. Böning, F. U. Schwarzkopf, and J. R. E. Lutjeharms, 2009b: Increase in Agulhas leakage due to poleward shift of Southern Hemisphere westerlies. *Nature*, **462**, 495–498, doi:10.1038/nature08519.
- Blanke, B., and P. Delecluse, 1993: Variability of the tropical Atlantic Ocean simulated by a general circulation model with two different mixed-layer physics. *J. Phys. Oceanogr.*, **23**, 1363–1388.
- Boebel, O., J. Lutjeharms, C. Schmid, W. Zenk, T. Rossby, and C. Barron, 2003: The Cape cauldron: A regime of turbulent inter-ocean exchange. *Deep-Sea Res. II*, **50**, 57–86.
- Böning, C. W., A. Dispert, M. Visbeck, S. R. Rintoul, and F. U. Schwarzkopf, 2008: The response of the Antarctic Circumpolar Current to recent climate change. *Nat. Geosci.*, **1**, 864–869, doi:10.1038/ngeo362.
- Caley, T., J. Giraudeau, B. Malaizé, L. Rossignol, and C. Pierre, 2012: Agulhas leakage as a key process in the modes of Quaternary climate changes. *Proc. Natl. Acad. Sci. USA*, **109**, 6835–6839, doi:10.1073/pnas.1115545109.
- Chelton, D. B., R. A. DeSzoeke, M. G. Schlax, E. N. Karim, and S. Nicolas, 1998: Geographical variability of the first baroclinic Rossby radius of deformation. *J. Phys. Oceanogr.*, **28**, 433–460.
- Cunningham, S. A., and R. Marsh, 2010: Observing and modeling changes in the Atlantic MOC. *Wiley Interdiscip. Rev.: Climate Change*, **1**, 180–191, doi:10.1002/wcc.22.
- Debreu, L., and E. Blayo, 2008: Two-way embedding algorithms: A review. *Ocean Dyn.*, **58**, 415–428, doi:10.1007/s10236-008-0150-9.
- Dencausse, G., M. Arhan, and S. Speich, 2010: Spatio-temporal characteristics of the Agulhas Current retroflexion. *Deep-Sea Res. I*, **57**, 1392–1405, doi:10.1016/j.dsr.2010.07.004.
- de Ruijter, W. P. M., A. Biastoch, S. S. Drijfhout, J. R. E. Lutjeharms, R. P. Matano, T. Pichevin, P. J. van Leeuwen, and W. Weijer, 1999: Indian–Atlantic interocean exchange: Dynamics, estimation and impact ring shedding. *J. Geophys. Res.*, **104** (C9), 20 885–20 910.
- Dijkstra, H. A., and W. P. M. de Ruijter, 2001: On the physics of the Agulhas Current: Steady retroflexion regimes. *J. Phys. Oceanogr.*, **31**, 2971–2985.
- Downes, S. M., S. Budnick, J. L. Sarmiento, and R. Farneti, 2011: Impacts of wind stress on the Antarctic Circumpolar Current fronts and associated subduction. *Geophys. Res. Lett.*, **38**, L11605, doi:10.1029/2011GL047668.
- Franzese, A. M., S. R. Hemming, S. L. Goldstein, and R. F. Anderson, 2006: Reduced Agulhas leakage during the Last Glacial Maximum inferred from an integrated provenance and flux study. *Earth Planet. Sci. Lett.*, **250**, 72–88, doi:10.1016/j.epsl.2006.07.002.
- , —, and —, 2009: Use of strontium isotopes in detrital sediments to constrain the glacial position of the Agulhas Retroflexion. *Paleoceanography*, **24**, PA2217, doi:10.1029/2008PA001706.
- Fyfe, J. C., and O. A. Saenko, 2006: Simulated changes in the extratropical Southern Hemisphere winds and currents. *Geophys. Res. Lett.*, **33**, L06701, doi:10.1029/2005GL025332.
- , —, K. Zickfeld, M. Eby, and A. J. Weaver, 2007: The role of poleward-intensifying winds on Southern Ocean warming. *J. Climate*, **20**, 5391–5400.
- Gent, P. R., and J. C. McWilliams, 1990: Isopycnal mixing in ocean circulation models. *J. Phys. Oceanogr.*, **20**, 150–155.
- Gordon, A. L., 1986: Inter-ocean exchange of thermocline water. *J. Geophys. Res.*, **91** (C4), 5037–5046.
- , R. F. Weiss, W. M. Smethie, and M. J. Warner, 1992: Thermocline and intermediate water communication between the South Atlantic and Indian Oceans. *J. Geophys. Res.*, **97**, 7223–7240.
- Graham, R. M., A. M. de Boer, K. J. Heywood, M. R. Chapman, and D. P. Stevens, 2012: Southern Ocean fronts: Controlled by wind or topography? *J. Geophys. Res.*, **117**, C08108, doi:10.1029/2012JC007887.
- Haidvogel, D. B., and A. Beckmann, 1999: *Numerical Ocean Circulation Modeling*. Series on Environmental Science and Management, Vol. 2, Imperial College Press, 344 pp.
- Hallberg, R., and A. Gnanadesikan, 2006: The role of eddies in determining the structure and response of the wind-driven Southern Hemisphere Overturning: Results from the Modeling

- Eddies in the Southern Ocean (MESO) project. *J. Phys. Oceanogr.*, **36**, 2232–2252.
- Hodgson, D. A., and L. C. Sime, 2010: Palaeoclimate: Southern westerlies and CO₂. *Nat. Geosci.*, **3**, 666–667, doi:10.1038/ngeo970.
- Knorr, G., and G. Lohmann, 2003: Southern Ocean origin for the resumption of Atlantic thermohaline circulation during deglaciation. *Nature*, **424**, 532–536, doi:10.1038/nature01855.
- Kohfeld, K. E., R. M. Graham, A. M. de Boer, L. C. Sime, E. W. Wolff, C. Le Quéré, and L. Bopp, 2013: Southern Hemisphere westerly wind changes during the Last Glacial Maximum: Paleo-data synthesis. *Quat. Sci. Rev.*, **68**, 76–95, doi:10.1016/j.quascirev.2013.01.017.
- Large, W. G., and S. G. Yeager, 2009: The global climatology of an interannually varying air–sea flux data set. *Climate Dyn.*, **33**, 341–364, doi:10.1007/s00382-008-0441-3.
- , J. C. McWilliams, and S. C. Doney, 1994: Oceanic vertical mixing: A review and a model with a nonlocal boundary layer parameterization. *Rev. Geophys.*, **32**, 363–403.
- Le Bars, D., W. P. M. de Ruijter, and H. A. Dijkstra, 2012: A new regime of the Agulhas Current retroflection: Turbulent choking of Indian–Atlantic leakage. *J. Phys. Oceanogr.*, **42**, 1158–1172.
- Madec, G., 2008: NEMO ocean engine. Note du Pole de Modelisation de l'Institut Pierre-Simon Laplace 27, 215 pp.
- , and M. Imbard, 1996: A global ocean mesh to overcome the North Pole singularity. *Climate Dyn.*, **12**, 381–388, doi:10.1007/BF00211684.
- Marchesiello, P., J. C. McWilliams, and A. Shchepetkin, 2001: Open boundary conditions for long-term integration of regional oceanic models. *Ocean Modell.*, **3**, 1–20, doi:10.1016/S1463-5003(00)00013-5.
- , L. Debreu, and X. Couvelard, 2009: Spurious diapycnal mixing in terrain-following coordinate models: The problem and a solution. *Ocean Modell.*, **26**, 156–169, doi:10.1016/j.oceanmod.2008.09.004.
- Marshall, J., and R. Plumb, 2007: *Atmosphere, Ocean and Climate Dynamics: An Introductory Text*. Academic Press, 334 pp.
- Meredith, M. P., and Coauthors, 2011: Sustained monitoring of the Southern Ocean at Drake Passage: Past achievements and future priorities. *Rev. Geophys.*, **49**, RG4005, doi:10.1029/2010RG000348.
- Oke, P., and M. England, 2004: Oceanic response to changes in the latitude of the Southern Hemisphere subpolar westerly winds. *J. Climate*, **17**, 1040–1054.
- Otto-Bliesner, B. L., E. C. Brady, G. Clauzet, R. Tomas, S. Levis, and Z. Kothavala, 2006: Last Glacial Maximum and Holocene climate in CCSM3. *J. Climate*, **19**, 2526–2544.
- Ou, H., and W. de Ruijter, 1986: Separation of an inertial boundary current from a curved coastline. *J. Phys. Oceanogr.*, **16**, 280–289.
- Peeters, F. J. C., R. Acheson, G.-J. Brummer, W. P. M. de Ruijter, R. R. Schneider, G. M. Ganssen, E. Ufkes, and D. Kroon, 2004: Vigorous exchange between the Indian and Atlantic Oceans at the end of the past five glacial periods. *Nature*, **430**, 661–665, doi:10.1038/nature02785.
- Penven, P., J. R. E. Lutjeharms, and P. Florenchie, 2006: Madagascar: A pacemaker for the Agulhas Current system? *Geophys. Res. Lett.*, **33**, L17609, doi:10.1029/2006GL026854.
- , P. Marchesiello, L. Debreu, and J. Lefèvre, 2008: Software tools for pre- and post-processing of oceanic regional simulations. *Environ. Model. Software*, **23**, 660–662, doi:10.1016/j.envsoft.2007.07.004.
- Pichevin, T., D. Nof, and J. R. E. Lutjeharms, 1999: Why are there Agulhas Rings. *J. Phys. Oceanogr.*, **29**, 693–707.
- Richardson, P. L., 2007: Agulhas leakage into the Atlantic estimated with subsurface floats and surface drifters. *Deep-Sea Res. I*, **54**, 1361–1389, doi:10.1016/j.dsr.2007.04.010.
- Ridgway, K. R., and J. R. Dunn, 2007: Observational evidence for a Southern Hemisphere oceanic supergyre. *Geophys. Res. Lett.*, **34**, L13612, doi:10.1029/2007GL030392.
- Rojas, M., and Coauthors, 2008: The Southern Westerlies during the last glacial maximum in PMIP2 simulations. *Climate Dyn.*, **32**, 525–548, doi:10.1007/s00382-008-0421-7.
- Rouault, M., P. Penven, and B. Pohl, 2009: Warming in the Agulhas Current system since the 1980's. *Geophys. Res. Lett.*, **36**, L12602, doi:10.1029/2009GL037987.
- Shchepetkin, A. F., and J. C. McWilliams, 1998: Quasi-monotone advection schemes based on explicit locally adaptive dissipation. *Mon. Wea. Rev.*, **126**, 1542–1580.
- , and —, 2005: The regional oceanic modeling system (ROMS): A split-explicit, free-surface, topography-following-coordinate oceanic model. *Ocean Modell.*, **9**, 347–404, doi:10.1016/j.oceanmod.2004.08.002.
- Sijp, W. P., and M. H. England, 2008: The effect of a northward shift in the Southern Hemisphere westerlies on the global ocean. *Prog. Oceanogr.*, **79**, 1–19, doi:10.1016/j.pcean.2008.07.002.
- , and —, 2009: Southern Hemisphere westerly wind control over the ocean's thermohaline circulation. *J. Climate*, **22**, 1277–1286.
- Smagorinsky, J., 1963: General circulation experiments with the primitive equations. I. The basic experiment. *Mon. Wea. Rev.*, **27**, 99–164.
- Son, S.-W., and Coauthors, 2010: Impact of stratospheric ozone on Southern Hemisphere circulation change: A multimodel assessment. *J. Geophys. Res.*, **115**, D00M07, doi:10.1029/2010JD014271.
- Speich, S., B. Blanke, and G. Madec, 2001: Warm and cold water routes of an OGCM thermohaline conveyor belt. *Geophys. Res. Lett.*, **28**, 311–314.
- Spence, P., J. C. Fyfe, A. Montenegro, and A. J. Weaver, 2010: Southern Ocean response to strengthening winds in an eddy-permitting global climate model. *J. Climate*, **23**, 5332–5343.
- Steele, M., R. Morfley, and W. Ermold, 2001: PHC: A global ocean hydrography with high-quality Arctic Ocean. *J. Climate*, **14**, 2079–2087.
- Swart, N. C., and J. C. Fyfe, 2012: Observed and simulated changes in the Southern Hemisphere surface westerly wind-stress. *Geophys. Res. Lett.*, **39**, L76711, doi:10.1029/2012GL052810.
- Taylor, K. E., R. J. Stouffer, and G. A. Meehl, 2012: An overview of CMIP5 and the experiment design. *Bull. Amer. Meteor. Soc.*, **93**, 485–498.
- The Drakkar Group, 2007: Eddy-permitting ocean circulation hindcasts of past decades. *CLIVAR Exchanges*, Vol. 12, International CLIVAR Project Office, Southampton, United Kingdom, 8–14.
- Toggweiler, J. R., J. L. Russell, and S. R. Carson, 2006: Midlatitude westerlies, atmospheric CO₂, and climate change during the ice ages. *Paleoceanography*, **21**, 1–15, doi:10.1029/2005PA001154.
- Tréguier, A.-M., 1992: Kinetic energy analysis of an eddy resolving, primitive equation North Atlantic model. *J. Geophys. Res.*, **97** (C1), 687–701.
- van Sebille, E., and P. J. van Leeuwen, 2007: Fast northward energy transfer in the Atlantic due to Agulhas rings. *J. Phys. Oceanogr.*, **37**, 2305–2315.

- , A. Biastoch, P. J. van Leeuwen, and W. P. M. de Ruijter, 2009: A weaker Agulhas Current leads to more Agulhas leakage. *Geophys. Res. Lett.*, **36**, L03601, doi:10.1029/2008GL036614.
- , P. J. van Leeuwen, A. Biastoch, and W. P. M. de Ruijter, 2010: Flux comparison of Eulerian and Lagrangian estimates of Agulhas leakage: A case study using a numerical model. *Deep-Sea Res. I*, **57**, 319–327, doi:10.1016/j.dsr.2009.12.006.
- Watson, P. G., D. J. Karoly, M. R. Allen, N. Faull, and D. S. Lee, 2012: Quantifying uncertainty in future Southern Hemisphere circulation trends. *Geophys. Res. Lett.*, **39**, L23708, doi:10.1029/2012GL054158.
- Weijer, W., and Coauthors, 2012: The Southern Ocean and its climate in CCSM4. *J. Climate*, **25**, 2652–2675.
- Wyrwoll, K.-H., B. Dong, and P. Valdes, 2000: On the position of Southern Hemisphere westerlies at the Last Glacial Maximum: An outline of AGCM simulation results and evaluation of their implications. *Quat. Sci. Rev.*, **19**, 881–898, doi:10.1016/S0277-3791(99)00047-5.
- Zahn, R., J. R. E. Lutjeharms, A. Biastoch, G. Knorr, W. Park, and C. J. C. Reason, 2010: Investigating the global impacts of the Agulhas Current. *Eos, Trans. Amer. Geophys. Union*, **91**, 109–110.
- Zalesak, S. T., 1979: Fully multidimensional flux corrected transport algorithms for fluids. *J. Comput. Phys.*, **31**, 335–362.